Acta Cryst. (1981). A37, 281–286

The Ultrastructure of Pyroxenoid Chain Silicates. III. Intersecting Defects in a Synthetic Iron–Manganese Pyroxenoid

BY D. A. JEFFERSON AND N. J. PUGH

Department of Physical Chemistry, Lensfield Road, Cambridge CB2 1EP, England

(*Received* 25 *July* 1980; *accepted* 1 *September* 1980)

Abstract

A synthetic pyroxenoid of nominal composition $MnFeSi_2O_6$ has been produced in the glassy state and examined by high-resolution electron microscopy after periods of annealing of from two to sixteen hours at 1070 K. Initially highly defective structures exhibiting large chain repeat distances are produced, but on further annealing the five-tetrahedra chain repeat of rhodonite predominates. (110)-type stacking faults are frequently observed. In most cases these faults involve considerable disruption of the lattice, but in certain instances the stacking fault displacement is equal to the rhodonite lattice repeat and the faults are visible only if the chain periodicity varies. In the latter case, the structure shows a two-dimensional ability to accommodate defects, and models for this, involving chain breaking and/or chain branching, are proposed.

Introduction

The presence of disordered intergrowths in various types of pyroxenoid chain silicates has been firmly established by high-resolution electron microscopy (Alario-Franco, Jefferson, Pugh & Thomas, 1980; Czank & Liebau, 1980; Ried & Korekawa, 1980) The original assignment of defects observed in (00*l*) lattice images to variations in the chain periodicity has been confirmed by combined computer simulation/electron-microscopic studies (Jefferson, Pugh, Alario-Franco, Mallinson, Millward & Thomas, 1980), and it is now possible to observe the tetrahedral arrangement in such structures directly (Smith, Jefferson & Mallinson, 1981), hence assigning chain repeats unambiguously. The existence of defects of the types reported confirms the original suggestion (Liebau, 1972) that the pyroxenoids form a continuous structural series, adapting to variations in cation size/pressure/temperature in a continuous manner. Transformations between different structural types have also been reported (Dent-Glasser & Glasser, 1961; Akimoto & Syono, 1972; Maresch & Mottana, 1976) and it has been assumed that variations in chain repeats within certain samples represent a situation where such transformations are frozen into the structure.

In addition to structural defects involving alterations in chain periodicity, other imperfections have also been reported in pyroxenoids. The most common of these are the (100) stacking faults observed in wollastonite (Jefferson & Thomas, 1975) which are believed to play a role in the polytypism of this silicate (Wenk, 1969). Analogous faults on (110) planes have been observed in pyroxferroite (Reiche, Messerschmidt & Bautsch, 1978) and rhodonite (Alario-Franco *et al.*, 1980), but these were comparatively rare and appeared to have no connection with the more common defects discussed above. Although variation in chain periodicity is believed to arise in the crystallization of silicates within the pyroxenoid group, with disordered intergrowths representing metastable states arising due to the extremely small energy differences between the various structural types (Czank & Liebau, 1980), direct evidence for this is lacking, owing to the fact that most previous studies have concentrated on the examination of naturally occurring specimens. In addition, the role of the less frequent stacking faults, if any, remains to be determined. As part of a systematic survey of structural chemistry within the metasilicate group, we describe here the results of a high-resolution electron-microscopic examination of a synthetic Fe/Mn pyroxenoid, and in particular the presence of certain defect structures which imply a hitherto unsuspected structural adaptability within this group of silicates.

Experimental

Synthetic preparations were carried out in a vacuum furnace at *ca* 1870 K and an operating vacuum of $6{\cdot}7 \times 10^{-5}$ Pa. Ferrous and manganous oxalates were finely ground with silica in the molecular ratio 1:1:2 and packed into Pt capsules, the lower end of which was welded, the upper end tightly crimped. These were then placed in a tungsten-spiral furnace and evacuated to better than $1{\cdot}3 \times 10^{-4}$ Pa. Gradual heating was then applied and pressure noted until complete decomposition of the oxalates had been achieved. The temperature was then gradually increased to at least 1870 K, the vacuum being maintained at $1{\cdot}3 \times 10^{-4}$ Pa or better throughout. Temperature measurement was by optical pyrometry. Owing to the very low viscosity

0567-7394/81/030281-06$01.00

of Mn–Fe–SiO_3 melts, which tended to escape from the platinum capsule, the capsule was placed such that its upper end protruded from the hot zone of the furnace. On quenching with argon gas after the run was complete a small globule of glassy material formed in the upper part of the capsule. This was finely ground and heated at *ca* 1070 K for periods of between two and sixteen hours. Upon completion of annealing, samples were again reground and deposited on holey carbon films in the normal manner.

Compositional analysis was carried out by examination of crushed fragments of the annealed specimens, supported on holey carbon films, in a Philips EM300 electron microscope fitted with a Link 860 energy-dispersive analytical system. Final mean composition determined in this way by the ratio method of Cliff & Lorimer (1972) was $Mn_{1.5}Fe_{0.7}Si_{1.8}O_6$. Considerable loss of Fe to the Pt capsule was noted, as in previous synthetic work (Ried & Korekawa, 1980), and, although the initial glassy quench product appeared to be relatively homogeneous, the final annealed samples often showed compositional variations of some 20% of any one element. For this reason annealing times of less than 2 h were not practicable.

High-resolution examination was carried out in a JEOL-200CX electron microscope, fitted initially with a side-entry goniometer stage of $C_s = 2{\cdot}5$ mm, this later being replaced by a top-entry goniometer with $C_s = 1{\cdot}2$ mm, giving a first zero on the phase contrast transfer function at the Scherzer focus (Erikson & Klug, 1971) of some 2·5 Å. Although the point-to-point resolution offered by this stage was such that individual SiO_4 tetrahedra could be imaged in the appropriate projection (Thomas & Jefferson, 1978) this was not the primary aim of the examination, as most of the defects observed were in relatively thick crystals. Micrographs were recorded at magnifications in the range 300 000–380 000, but the restricted specimen tilting ($\pm 10°$) prevented images of any one crystal from being recorded in more than one projection.

Results

Typical micrographs recorded from specimens of the annealed samples are illustrated in Fig. 1. For annealing times of eight hours or more, the five-tetrahedra repeat of rhodonite was found to be the equilibrium structure, with only very occasional defects present, crystal perfection generally extending over regions of at least 1000 Å (Fig. 1*a*). At the other extreme, however, for specimens annealed for only two hours, no one chain periodicity was characteristic of any crystal. Fig. 1(*b*) illustrates a typical micrograph, taken as part of a through-focal series, and selected, in the light of previous computer-simulated models of defects in these structures (Jefferson *et al.*, 1980), on the basis that the true structural periodicity was only apparent in thicker regions of crystals, at a defect of focus slightly greater than the Scherzer focus, such that spatial frequencies corresponding to longer periodicities would be imaged with the correct contrast. Chain periodicities of five, seven and nine tetrahedra are indicated in Fig. 1(*b*), and also one region where a defect of width corresponding to thirteen tetrahedra is visible. Defects of the latter type were relatively uncommon, and never occurred in regular fashion, in accordance with the predictions of Czank & Liebau (1980).

On increasing the annealing time to periods of four hours, the five-tetrahedra repeat of rhodonite was found to predominate, with longer periodicities becoming less common. In some crystals, however, the three-tetrahedra repeat of the wollastonite structure was evident, Fig. 2(*a*). Here quite an extensive region of this structure can be observed, although overall the rhodonite structure was most characteristic of the crystal, with

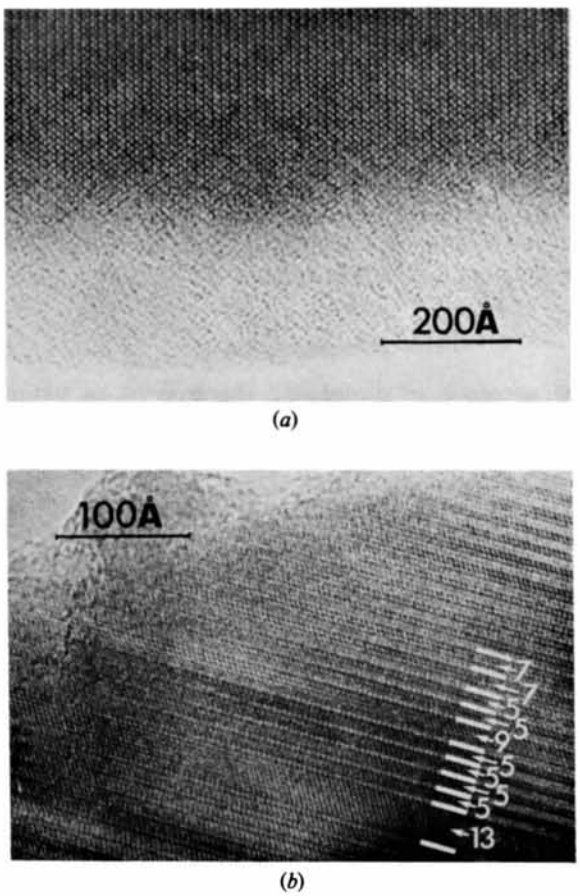

(*a*)

(*b*)

Fig. 1. (*a*) Typical lattice image of a crystal of synthetic $MnFeSi_2O_6$ (nominal) after eight hours annealing at 1070 K. (*b*) Lattice image of a crystal from the same specimen, but after only two hours annealing. The chain repeat distance (in numbers of SiO_4 tetrahedra) is shown on the latter. Both images were taken with the electron beam parallel to [100] of the rhodonite structure.

occasional seven-tetrahedra pyroxmangite defects. The micrograph of Fig. 2(*b*) illustrates some of the practical pitfalls of imaging these defect structures. As the structural perturbation on going from one repeat to another is only slight, careful examination at the highest resolution is necessary to observe structural changes at the margins of crystals, whereas in thicker regions multiple electron scattering highlights the true local periodicity.

Stacking faults in (110) planes of the matrix rhodonite were also observed, although never in samples annealed for more than four hours. One typical example is shown in Fig. 3, where, in the manner described previously (Alario-Franco *et al.*, 1980), such faults originate *within* the crystal and are distinguished by a gradually increasing offset of (00*l*) fringes intersecting them. Two features of the defect illustrated in Fig. 3 are immediately obvious, one being a virtual absence of any strain contrast normally associated with terminating defects. In addition, it is evident that this stacking fault has a definite width, which increases on moving from left to right along the fault, corresponding to the gradual increase of the (00*l*) fringe displacement. The crystal thickness in this region is <300 Å, as shown by the fact that the pyroxmangite defects labelled *A*, *B* and *C* are characterized by a 5 Å pair of fringes rather than by their true periodicity of 17·4 Å (Jefferson *et al.*, 1980), and consequently multiple-scattering effects will not dominate the image, and the stacking fault width must be regarded as a real effect.

The pyroxmangite defects in Fig. 3 follow the same pattern of offsets on crossing the stacking fault fringes in the rhodonite matrix, but this was not always the case, as indicated in Fig. 4. This shows a micrograph of a specimen annealed for only 2 h, and containing two (110) type stacking faults intersecting, within the area *ABCD*, a triplet and two pairs of pyroxmangite defects. At each stacking fault, fringes corresponding to the pyroxmangite repeats are offset, but in this case the magnitude of the offset corresponds to a five-tetrahedra rhodonite repeat. Consequently, fringes within the rhodonite matrix are unaffected, and except at the pyroxmangite defects, the stacking faults are not visible at all. Again, no strain contrast is evident. Fig. 4 also indicates a similar situation, with only a single stacking fault involved, intersecting a quadruplet and a single pyroxmangite defect within the region *EFGH*. In this latter case the offset, if measured in the same direction as in the area *ABCD*, corresponds to only two tetrahedra, but also, as the stacking fault passes through the quadruplet of pyroxmangite repeats, it is itself offset to the right by a distance of some 6·5 Å. Again, no strain contrast is evident, although in this case the stacking fault rapidly disappears as it moves into the crystal. Examples of such stacking faults which only perturbed the arrangement of pyroxmangite defects were relatively rare, but not unique, and had not been previously observed in natural pyroxenoids.

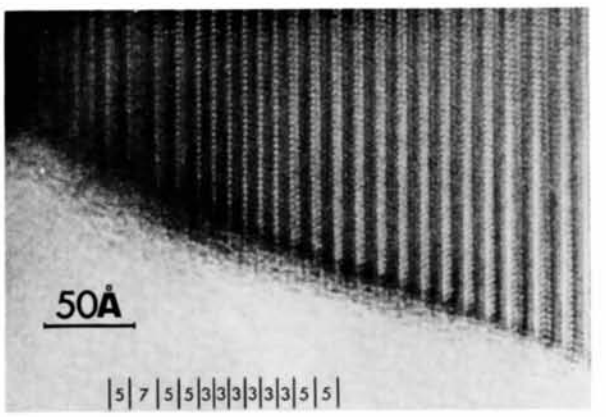

(*a*)

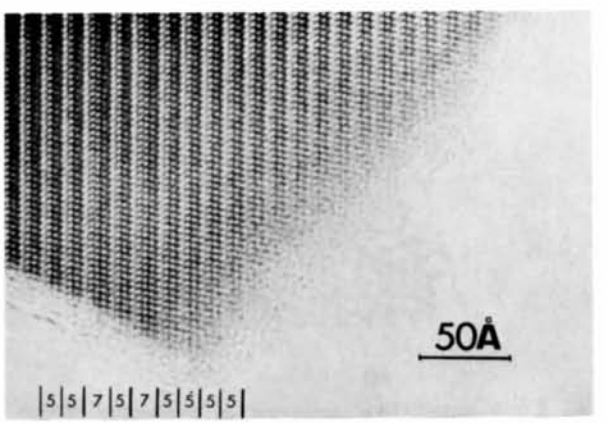

(*b*)

Fig. 2. (*a*) Lattice image of a crystal from a specimen annealed for four hours, the chain repeat distances (indicated) showing the presence of both wollastonite and pyroxmangite repeats within the rhodonite structure. (*b*) A thinner region of the same crystal, indicating the difficulty of observing defects in very thin regions. Electron beam parallel to [100].

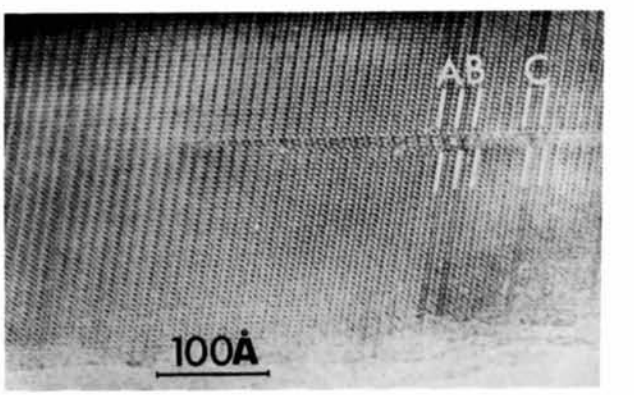

Fig. 3. Lattice image, taken with the electron beam parallel to [1$\bar{1}$0], of a stacking fault in a two-hour annealed specimen. Pyroxmangite defects crossing the fault are indicated at *A*, *B* and *C*.

Discussion

When micrographs from the specimens subjected to differing annealing times are compared with one another, the observed results are in good agreement with the predicted structural relationships in the pyroxenoid structures. At the annealing temperature of 1070 K, it appears that the rhodonite repeat is the equilibrium arrangement. The micrographs suggested, however, that initial crystallization begins with an arrangement closer to the pyroxene structure, where, in the nomenclature of Liebau (1972), the chain periodicity, although crystallographically expressed as a pair of tetrahedra, is in pyroxenoid terms an infinite one. On annealing this gradually transforms into shorter periodicities, repeats of nine tetrahedra or longer becoming virtually absent with annealing times of greater than two hours, almost all seven-tetrahedra pyroxmangite repeats being eliminated after eight hours. The appearance of wollastonite regions such as those illustrated in Fig. 2(*a*) remains more problematical, but it is possible that these represent a compromise arrangement where, in a region which has an equilibrium rhodonite structure, small areas of three- and seven-tetrahedra strips compensate for each other's presence. No evidence was found for the presence of pyroxmangite or wollastonite defects which terminated within the body of a crystal; consequently such defects must gradually be transported to the margins of crystals, along the whole of their length, and then shed from the structure. Although at first appearing unlikely, this is in accordance with the structure principles upon which the pyroxenoid structures are based, namely that the tetrahedral repeat in any part of a (00*l*) strip determines, *via* its complementary array of octahedrally coordinated cations, the chain repeat in an immediately adjacent area, and so on, throughout the crystal. It is perhaps significant that, in all cases where a pronounced crystal edge was parallel to (00*l*) planes, defects tended to be concentrated at this edge.

The cases of intersecting defects and stacking faults illustrated in Fig. 4 show the closest approach that the structure can apparently make to terminating a defect where a change in periodicity occurs. In these cases it would appear that some form of lattice strain would be essential. However, this need not be the case, as indicated in the structural diagram of Fig. 5. Fig. 5(*a*) gives a schematic representation of a pyroxmangite

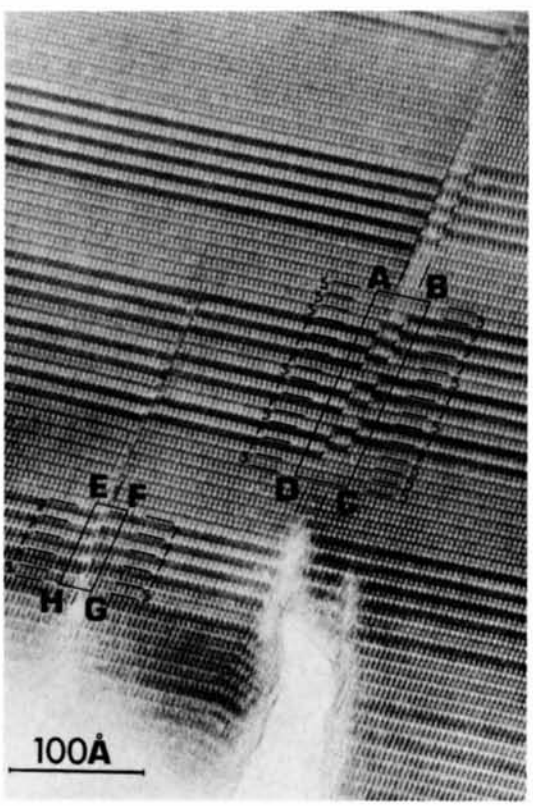

Fig. 4. Lattice image from a crystal of the same specimen as Fig. 3 and in the same orientation, indicating intersecting stacking faults and variations in chain periodicity. Areas *ABCD* and *EFGH* are discussed in the text.

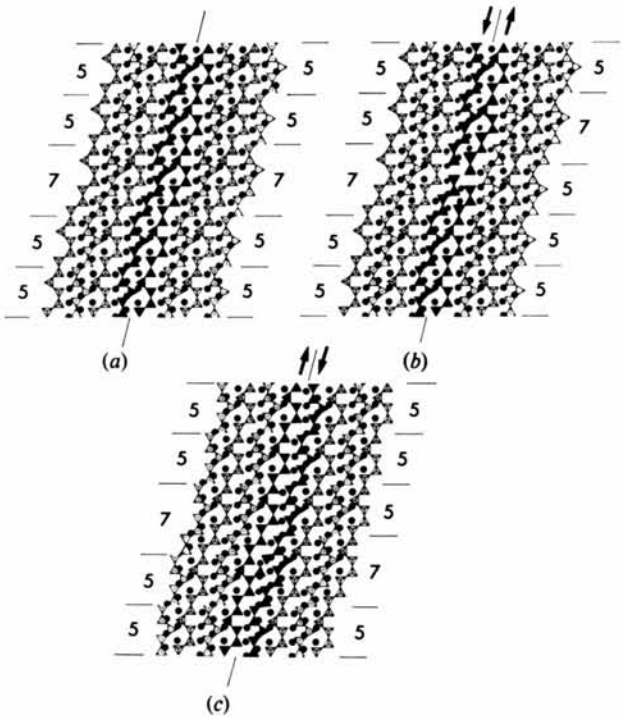

Fig. 5. Schematic [100] projection of intersecting defects in rhodonite. Rows of tetrahedra are shown as triangles (adjacent rows point alternately up and down) and octahedrally coordinated cations as filled circles. The chain repeats (in numbers of tetrahedra) are indicated and tetrahedra adjacent to the stacking fault plane are shown as filled triangles. (*a*) Stacking fault not in operation. (*b*) Stacking fault operating, with a net displacement of five tetrahedra along its plane. (*c*) A similar fault, but with the displacement in the opposite direction.

defect within a rhodonite matrix. For clarity the octahedral cations are indicated by filled circles and the actual octahedra, which are severely distorted, are not shown. Shaded tetrahedra indicate where a stacking fault is to be introduced. Fig. 5(*b*) shows the stacking fault in operation, the right-hand side of the arrangement being displaced upwards by five tetrahedra. The net effect of this is to bring the two chains bordering the stacking fault too close together, an arrangement which might be expected to produce considerable structural strain. This can however be avoided if chain breaking is permitted; in particular, if the unique tetrahedra in this pair of chains, which define the overall periodicity, are omitted, the two halves of this hypothetical crystal will fit together well. Some octahedral cation sites are also lost in the process, two complete formula units of the structure being shed and stoichiometry maintained. Fig. 5(*c*) indicates the alternative displacement model. Here the right-hand side is shifted downward by five tetrahedra with respect to the left. The net effect of this is to move the two chains bordering the fault further apart. Again, the resulting misfit can be accommodated, but in this case by introducing two additional formula units into the structure and, in effect, allowing the metasilicate chains to branch. These are not the only possibilities, but they do offer the most structurally satisfying solution.

Fig. 6 indicates how the principles outlined above can be applied to the former of the two sets of intersecting defects illustrated in Fig. 4. In this case, as the displacement at the stacking faults is in an upward direction on going from left to right, by a vector corresponding to five tetrahedra, then the case of Fig. 5(*b*) applies and chain breaking is necessary. If this is permitted, then a pair of chains bordering each stacking fault is broken at each pyroxmangite-like defect; consequently there are seven such breaks along each stacking fault, but overall stoichiometry and coherence with the rhodonite matrix is maintained. In the second of the cases of intersecting defects shown in Fig. 4, the net displacement across the fault is equivalent to a downward shift of five tetrahedra, and the model of Fig. 5(*c*) can be applied to the region *EFGH*. The resulting structural model is illustrated in Fig. 7. In a similar fashion to the former case, chain modification occurs at every pyroxmangite strip, the modification in this case being that of chain branching. The model in Fig. 7, however, is complicated by the fact that the stacking fault itself side-steps, in the lower part of region *EFGH*, and although this makes no difference to the manner in which offsets of chain periodicity defects are accommodated, further chain modification is also necessary. The simplest way in which this can be done is by inserting, at the point where the stacking fault is itself offset, a nine-tetrahedra ferrosilite III repeat in place of the pyroxmangite repeat present in adjacent chains. Again, the required number of cations is also readily accommodated, and full stoichiometry can be maintained. In such instances where both stacking faults and variations in chain periodicity are simultaneously offset, the parent structure proves to be adaptable in two dimensions rather than the one-dimensional adaptability previously found.

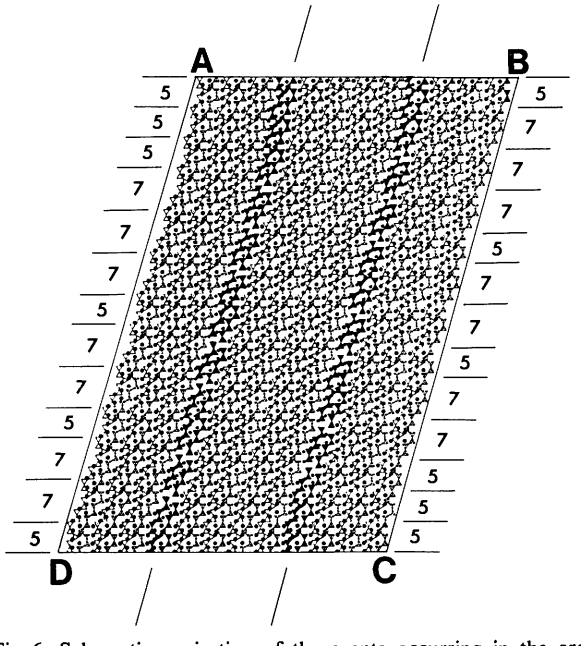

Fig. 6. Schematic projection of the events occurring in the area *ABCD* of Fig. 4. The lines of the two stacking faults are indicated, and tetrahedra adjacent to these faults are again shown as filled triangles.

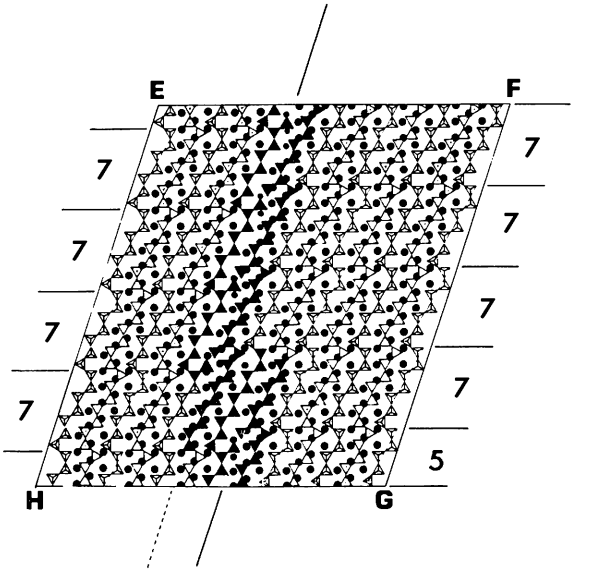

Fig. 7. A similar projection to that of Fig. 6, but here depicting the events occurring in area *EFGH*. In this case both the lines of the stacking fault and their offset are indicated.

Conclusions

The results described above indicate two important features of silicates in the pyroxenoid group. As was previously supposed, crystallization of these structures is, in effect, a continual process where the structure type adopted gradually changes as the temperature is lowered, *via* a series of disordered intergrowth structures, to an equilibrium, or near-equilibrium arrangement. The material appears to adapt continually in the crystallization process, by means of metastable intermediate states, until the appropriate structural type is attained, with no evidence of the more normal nucleation and growth from the initial glassy product.

The most surprising feature indicated by these results, however, is in the degree of structural adaptability shown. In particular, no previous evidence for intersecting defects which appear to involve so little structural strain has been noted: these defect structures, which almost certainly involve breaking or branching of the metasilicate chains, suggest that the adaptability of these chains to thermodynamic and kinetic factors is far greater than was previously suspected. Subsequent results in the $(Mg,Mn)SiO_3$ structures (Pugh & Jefferson, 1981) have shown this even more clearly, especially if still shorter annealing times are used. It is interesting to speculate whether this behaviour will enable these silicates to form metastable states even in the very initial stages of crystallization from the glass.

The authors acknowledge the support of the SRC, for providing the JEOL 200CX electron microscope and a CASE studentship to NJP. The advice and encouragement of Professor J. M. Thomas, FRS is also gratefully acknowledged.

References

AKIMOTO, S. I. & SYONO, Y. (1972). *Am. Mineral.* **57**, 76–84.
ALARIO-FRANCO, M., JEFFERSON, D. A., PUGH, N. J. & THOMAS, J. M. (1980). *Mater. Res. Bull.* **15**, 73–79.
CLIFF, G. & LORIMER, G. W. (1972). *Proc. Vth Eur. Congr. Electron Microsc.* pp. 140–143.
CZANK, M. & LIEBAU, F. (1980). *Phys. Chem. Minerals.* In the press.
DENT-GLASSER, L. S. & GLASSER, F. P. (1961). *Acta Cryst.* **14**, 818–822.
ERIKSON, H. P. & KLUG, A. (1971). *Philos. Trans. R. Soc. London Ser. B*, **261**, 105–118.
JEFFERSON, D. A., PUGH, N. J., ALARIO-FRANCO, M., MALLINSON, L. G., MILLWARD, G. R. & THOMAS, J. M. (1980). *Acta Cryst.* A**36**, 1058–1065.
JEFFERSON, D. A. & THOMAS, J. M. (1975). *Mater. Res. Bull.* **10**, 761–768.
LIEBAU, F. (1972). *Handbook of Geochemistry*, Vol. II, Ch. 14. Belin: Springer-Verlag.
MARESCH, W. V. & MOTTANA, A. (1976). *Contrib. Mineral. Petrol.* **55**, 69–79.
PUGH, N. J. & JEFFERSON, D. A. (1981). In preparation.
REICHE, M., MESSERSCHMIDT, A. & BAUTSCH, H. J. (1978). *Geol. Wiss. Berlin*, **6**, 709–718.
RIED, H. & KOREKAWA, M. (1980). *Phys. Chem. Minerals*, **5**, 351–365.
SMITH, D. J., JEFFERSON, D. A. & MALLINSON, L. G. (1981). *Acta Cryst.* A**37**, 273–280.
THOMAS, J. M. & JEFFERSON, D. A. (1978). *Endeavour*, **2**, 127–136.
WENK, H. R. (1969). *Contrib. Mineral. Petrol.* **22**, 238–247.

Acta Cryst. (1981). A**37**, 286–292

The Three-Colored Three-Dimensional Space Groups

BY DAVID HARKER

Medical Foundation of Buffalo, Inc., 73 High Street, Buffalo, NY 14203, USA

(*Received* 15 *May* 1980; *accepted* 9 *October* 1980)

Abstract

This article contains a table of the groups of combined geometrical and color-permutational symmetry operations that leave a certain kind of three-colored, three-dimensionally periodic object apparently unchanged. The asymmetric units – 'motifs' – of the object are all either geometrically congruent to, or are mirror images of, one another. Each motif has a 'color' representing a scalar quality of some kind, and three different colors of motifs are assumed to occur in the object. Two types of three-colored space groups exist: type I in which all of the geometrical lattice translations leave all the motifs unchanged in color, and type II in which at least one of the geometrical lattice translations requires a permutation of the three colors in order to restore the original appearance. There are 88 three-colored space groups of type I, and 341 of

0567-7394/81/030286-07$01.00